Scalp EEG-Based Pain Detection Using Convolutional Neural Network

Duo Chen, *Member, IEEE*, Haihong Zhang, Perumpadappil Thomas Kavitha, Fong Ling Loy, Soon Huat Ng, Chuanchu Wang, Kok Soon Phua, Soon Yin Tjan, Su-Yin Yang, and Cuntai Guan, *Fellow, IEEE*

***Abstract*— Pain is an integrative phenomenon coupled with dynamic interactions between sensory and contextual processes in the brain, often associated with detectable neurophysiological changes. Recent advances in brain activity recording tools and machine learning technologies have intrigued research and development of neurocomputing techniques for objective and neurophysiology-based pain detection. This paper proposes a pain detection framework based on Electroencephalogram (EEG) and deep convolutional neural networks (CNN). The feasibility of CNN is investigated for distinguishing induced pain state from resting state in the recruitment of 10 chronic back pain patients. The experimental study recorded EEG signals in two phases: 1. movement stimulation (MS), where induces back pain by executing predefined movement tasks; 2. video stimulation (VS), where induces back pain perception by watching a set of video clips. A multi-layer CNN classifies the EEG segments during the resting state and the pain state. The novel approach offers high and robust performance and hence is significant in building a powerful pain detection algorithm. The area under the receiver operating characteristic curve (AUC) of our approach is 0.83 ± 0.09 and 0.81 ± 0.15, in MS and VS, respectively, higher than the state-of-the-art approaches. The sub-brain-areas are also analyzed, to examine distinct brain topographies relevant for pain detection. The results indicate that MS-induced pain tends to evoke a generalized brain area, while the evoked area is relatively partial under VS-induced pain. This work may provide a new solution for researchers and clinical practitioners on pain detection.**

***Index Terms*— Pain detection, chronic pain, EEG, CNN.**

Manuscript received July 3, 2021; revised December 29, 2021; accepted January 19, 2022. Date of publication January 28, 2022; date of current version February 9, 2022. *(Corresponding authors: Su-Yin Yang; Cuntai Guan.)*

This work involved human subjects or animals in its research. Approval of all ethical and experimental procedures and protocols was granted by the National Healthcare Group Domain Specific Review Board under Approval No. NHG DSRB 2016/00516.

Duo Chen is with the School of Artificial Intelligence and Information Technology, Nanjing University of Chinese Medicine, Nanjing 210023, China, and also with the School of Computer Science and Engineering, Nanyang Technological University, Singapore 639798 (e-mail: 380013@njucm.edu.cn; chenduo@ntu.edu.sg).

Haihong Zhang, Soon Huat Ng, Chuanchu Wang, and Kok Soon Phua are with the Institute for Infocomm Research, A*STAR, Singapore 138632 (e-mail: hhzhang@i2r.a-star.edu.sg; shng@i2r.a-star.edu.sg; ccwang@i2r.a-star.edu.sg; ksphua@i2r.a-star.edu.sg).

Perumpadappil Thomas Kavitha and Cuntai Guan are with the School of Computer Science and Engineering, Nanyang Technological University, Singapore 639798 (e-mail: ptkavitha@ntu.edu.sg; ctguan@ntu.edu.sg).

Fong Ling Loy is with The Physio Movement, Singapore 238164 (e-mail: loyfongling@gmail.com).

Soon Yin Tjan and Su-Yin Yang are with the Tan Tock Seng Hospital, Singapore 308433 (e-mail: soon_yin_tjan@ttsh.com.sg; su_yin_yang@ttsh.com.sg).

Digital Object Identifier 10.1109/TNSRE.2022.3147673

I. Introduction

PAIN, a vital phenomenon that depends on the dynamic integration of sensory and contextual processes, is one of the top causes of disability, and if untreated, it can lead to undesirable personal and sociological outcomes, such as depression, work absenteeism, and presenteeism, and unnecessary costs to families and caregivers [1], [2]. The International Association for the Study of Pain (2020) has defined pain as an "unpleasant sensory and emotional experience associated with, or resembling that associated with, actual or potential tissue damage" [3], and compels people to seek healthcare [4]. Despite the tremendous growth in medical diagnosis and treatment technologies, there is still an urgent need for accurate chronic pain detection or pain management [5]. Recent advances in brain imaging technologies have led to neurocomputational models that use neurological signals to classify pain states. These models make use of the alterations in structure and functionalities of the chronic pain patient's brain. Models based on Electroencephalogram (EEG) data in the literature associate specific neuronal activities in the motor cortex with different pain states [6], [7]. Compared to fMRI, which is also widely used for functional recording, the electroencephalography (EEG) to predict brain function abnormalities and extract a brain-based marker of chronic pain is particularly appealing as the system is non-invasive, cost-effective, broadly available, and potentially mobile [8]. Besides, EEG is deemed more sensitive for registering the complex interplay of different brain functional processes occurring in timespans of milliseconds, such as pain. Hence, the goal of the current study is to detect pain states in chronic pain patients based on neural signatures extracted from EEG signals. This work is motivated by constructing an objective generalizable computer-aided machine learning model to achieve reliable pain detection accuracy. Results in this work might not only be helpful for the diagnosis and classification of chronic pain in a less expensive and more comfortable manner, but might also represent a target for

novel therapeutic strategies such as neurofeedback [9], or non-invasive brain stimulation techniques [10].

It is reported that in chronic pain, the adaptive integration of sensory and contextual processes is severely disturbed [1]. This disturbed integration is associated with significant structural and functional changes of the brain [11], [12], which can be tracked effectively using EEG [13]–[15]. Only a few EEG studies have attempted to address the observable chronic pain-related cortical activity adequately. Yet, their results are not fully consistent [7]. An increase of theta and gamma oscillations in chronic pain patients is one of the abnormalities reported [16], whereas reductions in alpha and beta power have been presented [13]. However, these abnormal theta oscillations were not observed in other studies [15]. Although previous studies have taken a few preliminary steps towards inventing an efficient brain-based marker of chronic pain [17], [18], there are very limited attempts for objective EEG-based pain detection classifying induced pain EEG vs. resting-state EEG [19], [20]. Such data would be helpful to prevent, diagnose, and treat painful conditions [21], [22]. However, evidence from EEG studies remains weak.

Machine learning has been fundamental for the success of neuroimaging techniques associated with pain [5]. It can better interpret the complexity of pain by revealing patterns in clinical and experimental data, by obtaining usable information that is essential to acquire new knowledge. In pain-related classification problems, machine learning makes use of pain-related data to create a mapping of features and to learn a signature of pain (or class). In the past few decades, Convolutional Neural Network (CNN) has shown its great potential in multiple fields such as computer vision and speech recognition [23]. This method is suitably scaled for large datasets, as a hierarchical structure in natural signals can be exploited. As such, CNN appears especially suitable for analyzing the long-term, high dimensional, high non-stationary signals, like EEG. Several studies have explored the application of CNN for EEG analysis within the healthy population in the areas of sensory processing, cognitive-emotional processing, speech, motor planning/execution, and have achieved great performance [24]–[27].

CNN may have proven its huge potential on the aforementioned EEG classification problems. However, there is very limited work of using CNN for EEG-based chronic pain detection; a challenging but vital task in pain diagnosis and treatment for current and future purposes. Motivated by this fact, a multi-layered framework using CNN is proposed in this study for EEG-based chronic back pain detection. The proposed system studies pain data of 10 chronic back pain patients and achieves better Area under the Receiver Operating Characteristic Curve (AUC) in pain detection than the state-of-the-art methods. The experimental results indicate that the proposed study is establishing a guideline for using CNN in EEG-based pain detection with high accuracy. To the best of our knowledge, this is the first attempt to use deep CNN to construct an objective EEG-based pain detection for chronic pain.

II. Experimental Setup

The experiment was conducted at Tan Tock Seng Hospital (TTSH), Singapore, with ethics approval from the National Healthcare Group Domain Specific Review Board (NHG DSRB 2016/00516). A total of 10 (6 lower-back pain patients and 4 back pain patients) volunteer participants were recruited. The experiment involved these subjects performing two distinctive sets of carefully-designed tasks: Movement Stimulation (MS) tasks and Video Stimulation (VS) tasks. The IDs of the subjects hereinafter referred to as sub01, sub02, sub03, etc. The study will examine the sensitivity of the EEG-based method described above in detecting significant differences in brain signals in patients with chronic pain. Participants were recruited via the pain management clinic; inter-hospital department study recruitment invites in TTSH and via the pain management clinic website. A total of 2 visits to the study site (pain management clinic, TTSH) over two consecutive weeks were required, each taking approximately 1 hour 15 minutes. The first session involved a doctor's office visit for a screening assessment prior to study participation. Participants then participate in two different sets of non-invasive experimental conditions one after another, i.e., MS and VS.

The Photograph Series of Daily Activities (PHODA) [28] specifically retrieves a patient's associations between certain movements and expectations of harm and (re)injury, and it taps therefore into the threat value of daily activities. The original version of this tool was developed consisting of photos of 8 possible movements (lifting, bending, turning, reaching, falling, intermittent load, unexpected movement, long-lasting load instance, or sit with limited dynamics), which were derived from basic movements (extending, inflecting, rotating, lateral inflecting, compression and traction) and 2 manners of moving (static and dynamic). These 8 movements were then set against 4 areas of daily occupations (activities of daily living, housekeeping, work and sport, and leisure time) and converted into recognizable and frequent activities instead of their biomechanics. The resulting list of movements and activities was tested, corrected, and supplemented by several experts in the area of low back pain (human movement scientists, physical therapists, and psychologists). This resulted in the 98 item PHODA, which has a shortened version of a selection of 40 items. Test-retest reliability and construct validity support PHODA's value as an instrument to determine the threat value of activities in chronic low back pain patients.

This study created videos of 15 out of the 40 activities identified in the PHODA- selection of the 15 activities based on movements that patients will engage in on a daily basis in the local Singapore context. The VS is a kind of virtual stimulation. In order to simulate the daily scenes, we also designed the physical movement stimulation, i.e., MS.

The MS set consisted of a series of 15 physical movements simulating different daily tasks. Examples of the tasks are lifting and placing a loaded box, transferring dumbbells between two boxes, walking/jogging on a treadmill, and pushing a trolley, as shown in Fig. 1a. The time structure of an MS task is illustrated in Fig. 2a. An MS task began with 30 seconds resting (in stand-still position) period for the acquisition of

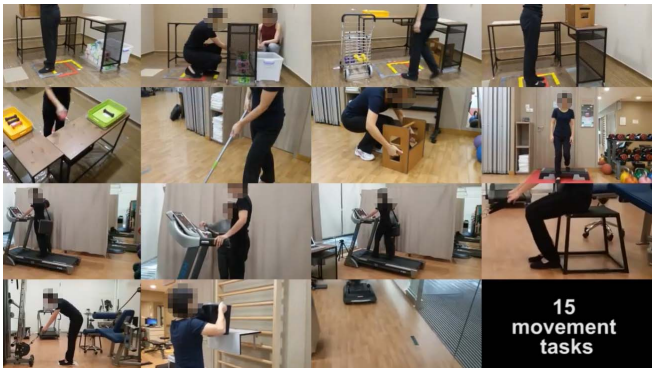

(a) Movement Tasks in MS

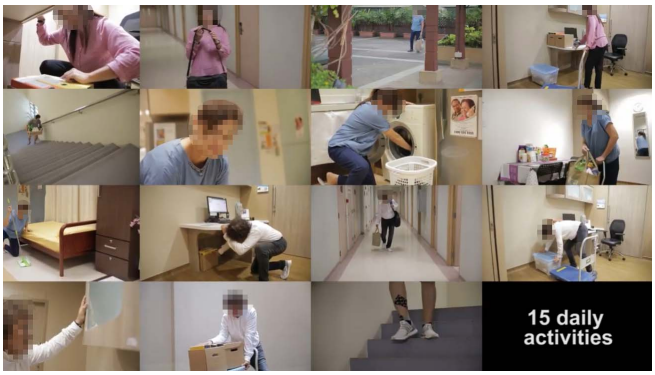

(b) Videos of Daily Activities in VS

Fig. 1. **Tasks in MS and videos in VS.** (a) depicts movement tasks employed in MS phase whereas (b) shows the videos watched by the patient, to induce pain episodes. In MS, the patient executes a series of 15 movement tasks (i.e., lifting a box up-and-down, move dumbbells between two boxes, jogging on a running machine, etc.) one by one. In VS, the patient sits still and watches a series of 15 short videos relates to pain scenes in daily activities one by one.

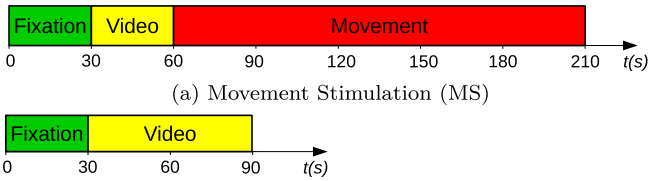

(a) Movement Stimulation (MS)

(b) Video Stimulation (VS)

Fig. 2. **Timing protocol of the two paradigms.** (a) Movement stimulation (MS) and (b) video stimulation (VS). In movement stimulation (MS): At the beginning of a trial (t = 0 s), a fixation hint appears on the black screen. The patient needs to stand still for 30 seconds (greed bar). Then, a 30s instruction video clip (yellow bar) plays back to illustrate the movement to perform. A hint appears on the screen at the end of the video and gives the order to execute a movement task (red bar). In video stimulation (VS): At the beginning of a trial (t = 0 s), a fixation hint appears on the black screen (green bar). The patient needs to sit still for 30 seconds. Then, the patient needs to watch a VS video clip that may induce pain (yellow bar). A 2s short break is set between trials in each stimulation.

resting-state EEG. The MS task then played back an instruction video clip of 30 seconds about the physical activity the subject needs to perform. The subject then performed such a task for a number of repetitions depending on the health condition. The numbers of repetitions for the 10 participants were 4,4,3,1,1,3,4,3,4, and 2, both in MS and VS.

The VS set consisted of watching a collection of 15 video footages of professional actors acting scenes of daily activities known to induce lower back and lower limb pain in chronic pain patients [28], as shown in Fig. 1b. The time structure of a VS task is illustrated in Fig. 2b. It also began with 30 seconds resting (in a seated position) period for the acquisition of resting-state EEG. The subject then watched the pain video clip.

Note that the "Movement" duration in Fig. 2a and the "Video" duration in Fig. 2b are for illustration purposes. The actual duration depends on the complexity of the motion, and the possible pain episode that may arise during the stimulation.

When the subject experienced a significantly elevated level of pain induced by the tasks above, the following mechanism was used to record the particular event. The subject immediately reported the onset of the pain to the physiotherapist who then registered this event using the data collection hardware and software, and at the same time instructed the patient to remain still for 20 seconds – this allowed recording of motion-artifact-free EEG during the period of induced pain. The series of tasks would be suspended until the induced pain was naturally relieved.

A special compact sensing device was developed by the Institute for Infocomm Research (I2R) team to capture the dynamics of electrophysiological signals during pain-inducing tasks. The device was integrated into a backpack with power and data connection to a computer via an extended USB cable. The subject could comfortably wear the sensor backpack while performing all the physical movements. The device used a Neuroscan NuAmps bio-potential amplifier to simultaneously measure 32 monopolar EEG potentials (i.e. 32 channels) and electrocardiogram (ECG) and Galvanic Skin Response (GSR). The ground electrode was at AFz, while the (A1 + A2)/2 was used as the reference channel. A1/2 was attached to the left/right mastoid. ECG and GSR were not considered in this particular report. The EEG channels followed the 10-20 system: Fp1, Fp2, F3, Fz, F4, F7, F8, FT7, FT8, T7, T8, TP7, TP8, FC3, FCz, FC4, C3, Cz, C4, CP3, CPz, CP4, P3, Pz, P4, P7, P8, PO1, PO2, O1, Oz and O2. All the EEG channels were measured using Neuroscan's gel-based QuikCap electrode system. A band-pass filter ($[0.5Hz, 100Hz]$) and a $50Hz$ notch filter were enabled in the amplifier to eliminate/reduce unwanted noises/interferences out of the range of interesting EEG rhythms. The EEGs were continuously recorded throughout MS and VS.

III. Methodology

In order to classify EEG features associated with the rest and pain states of each patient, a multi-layered neural network architecture is proposed here. Fig. 3 indicates the flowchart of EEG-based pain detection using CNN. First, data of N subjects are recorded using a multi-channel EEG amplifier. Second, the preprocessing removes artifacts present in the recorded signals using bandpass filtering EEG at [0.5, 100] Hz and using Independent Component Analysis (ICA). Third, the corrected EEG output of the preprocessing module is then segmented by a 5 seconds sliding window with 4 seconds

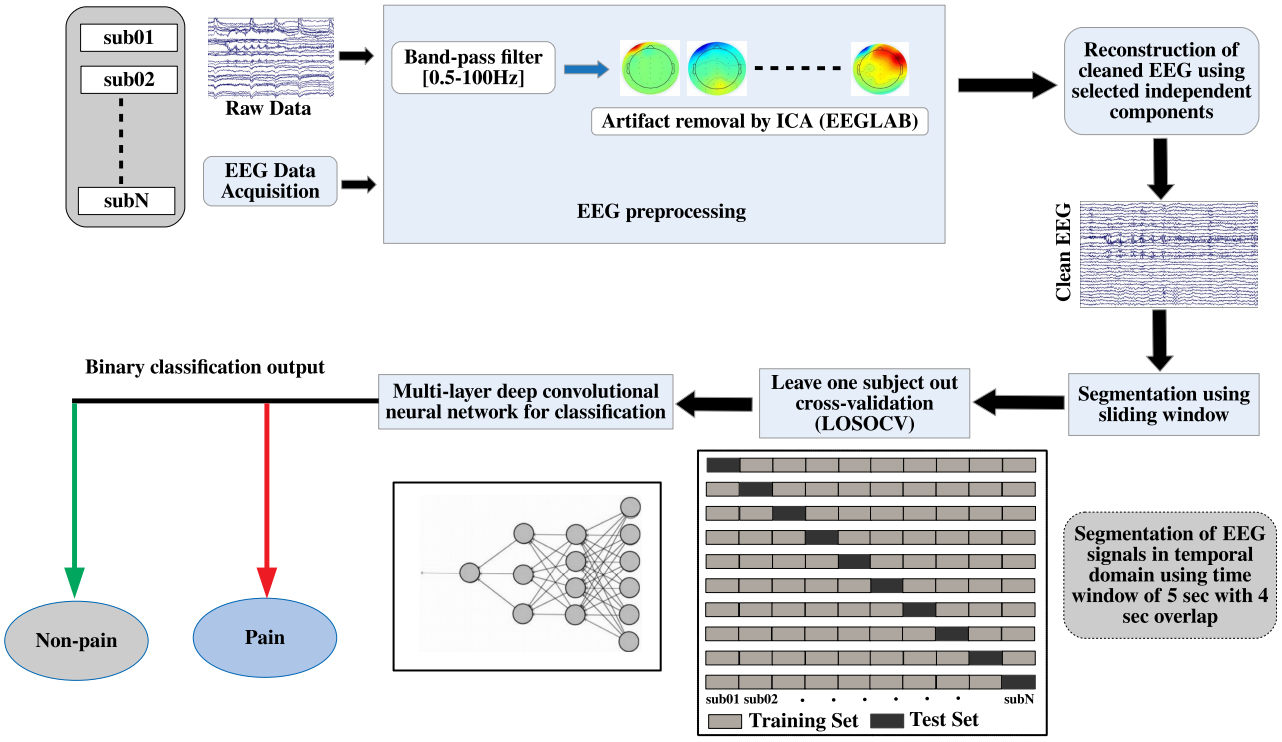

Fig. 3. **Flowchart of the proposed method for EEG-based pain detection.** The raw data recorded from the patient's brain is classified as "Pain" or "Non-pain" states using the proposed multi-layer CNN architecture in LOSOCV paradigm. Data of N subjects are imported. In block "Preprocessing", the raw EEG was firstly bandpass filtered at $[0.5, 100]Hz$. Then, ICA is used to remove artifacts. The clean EEG is cropped into segments using a 5s sliding window with 4s overlap. Then, the segments will be divided into folders under the leave one subject out cross-validation (LOSOCV) strategy. $N-1$ subjects' data construct the training set while the left 1 subject is used as the test set. Each subject is selected as the test set once representing a LOSOCV. Deep CNN is utilized to distinguish the segments. For space sake, the network is just a symbolic demonstration here. Details of the network structure are given in Section III-E. Each EEG segment is predicted into a certain class, i.e., "Pain", or "Non-pain."

overlapping. Then, the segmented EEG is classified using "Leave-one-subject-out Cross-Validation (LOSOCV)", where $N-1$ subjects' data is used for constructing the CNN model whereas the remaining one subject's data is used as a test set. Each subject is selected as the test set once representing a LOSOCV. The network shown is a symbolic demonstration of the network used. Details of the network structure are given in Section III-E. The Final output stage predicts the label of the segmented EEG as either i.e., "Pain", or "Non-pain". Details of each module and functionalities are explained in the sequel.

A. Data Acquisition

EEGs were acquired from all patients as per the timing protocol mentioned in Section II. In the MS phase, patients stood in front of the PC while recording EEG whereas, in VS phase, patients sat on a comfortable chair watching the pain-inducing videos. However, the recorded EEG signals may contain artifacts arising from movements of muscle and eye, which were then removed using the subsequent steps for preprocessing. In this work, pain detection is formulated into a binary classification problem: classifying "Pain" and "Non-pain" EEG from multi-channel scalp EEG recordings. "Pain" EEG is defined as pain episodes marked by the therapist in MS whereas physical experience is marked by the patient itself in VS. "Non-pain" EEG is defined as the EEG recordings in the fixation stage. To avoid certain artifacts that may be generated by movement, the patient was instructed to stand still for 30 seconds during fixation, and 20 seconds when a pain episode occurs in MS. In VS, the patient had to sit still entirely.

B. Preprocessing

The raw EEG was bandpass filtered at frequency band $[0.5, 100]Hz$ to remove very high-frequency components and to perform DC-removal. ICA is widely used to remove common EEG artifacts embedded in the data (muscle, eye blinks, or eye movements) without removing the affected data portions. To explore the high intelligence of CNN in pain detection, the manual intervention in preprocessing was minimized to keep the originality of the data by doing only bandpass filtering and ICA. The ICA component rejection followed the ICA artifact removal instruction of EEGLAB (https://eeglab.org/tutorials/06_RejectArtifacts/RunICA.html). Fig. 4 demonstrates an EEG before (blue lines) and after (red lines) an eye blink component removal. The EEG segment (blue lines) contains two eye blinks at seconds 0.6 and 3.5 and is clean (red lines) after the eye blink component is removed.

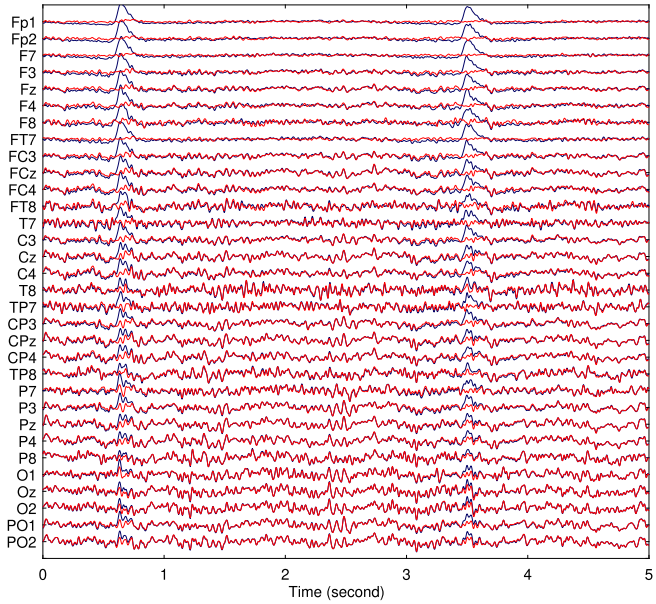

Fig. 4. **Example for artifact removal.** The EEG segment (blue lines) contains two eye blinks at seconds 0.6 and 3.5 and is clean (red lines) after the eye blink ICA component is removed.

C. Segmentation

In the proposed pain assessment approach, it is worth considering the fact that the duration and severity of pain vary among different patients. In order to ensure the credibility of "Pain" among patients, only the 10 seconds after every pain marker was used as a "Pain" episode for each subject in both phases. Hence for classification purposes, the long-term EEG was separated into 5 seconds length segments with 4 seconds overlapping. Fig. 5 demonstrates the "Pain" and "Non-pain" segmentations in MS and VS. In MS and VS, the fixation is treated as "Non-pain", while 10 seconds after a pain marker is treated as the "Pain". In Fig. 5, in each rest state (fixation) and pain state, a sliding window will split the long-term EEG into 5s segments.

Given a multi-channel EEG dataset X of patient $i \in \{1, 2, \ldots, N\}$, where N is the number of patients. Each dataset is divided into segments as described above. Concretely, we are given dataset $D^i = (X^1, y^1), (X^2, y^2), \ldots, (X^{N_i}, y^{N_i})$, where N_i denotes the total number of segments for patient i. The jth EEG segment $X^j \in \mathbb{R}^{C.T}, 1 \leq j \leq N_i$ contains C channels and T time points per segment, where $C = 32$ and $T = 5{*}250 = 1250$, in this study. The class label of segment j is denoted by $y^j \in \{0, 1\}$, where 0 represents "Non-pain" whereas 1 represents "Pain".

The number of pain episodes varies across patients. Table I lists a summary of the pain occurrence and segments of 10 patients involved in this study. Pain occurrence is marked either by the patient or therapist depending on the pain stimulation phase and the number of occurrences for each subject is listed in Table I. While considering the pain markers, multiple pain markers with intermittent gaps of less than 10 seconds will be considered as a single occurrence. The third column "Number of Segments" is after splitting each single-trial EEG into 5 seconds segments. The final column "Balanced" is the number of segments after oversampling. Oversampling is performed to avoid the possible trouble caused by data imbalance (due to the unbalanced number of "Pain" or "Non-pain" EEG segments) [29]. If the number of "Non-pain" and "Pain" segments are M and L respectively with $M \gg L$ for a particular subject, the sample size L is raised by randomly repeating "pain" copies to expand the sample size to M.

TABLE I
PAIN OCCURRENCE AND NUMBER OF SEGMENTS OF EACH PATIENT

	Occurrence		Number of Segments		Balanced	
ID	MS	VS	MS	VS	MS	VS
sub01	4	18	29	130	78	332
sub02	6	NaN*	44	-	116	-
sub03	2	2	16	6	78	26
sub04	2	2	14	12	52	44
sub05	22	16	139	126	337	222
sub06	30	49	187	387	531	756
sub07	4	5	28	30	28	30
sub08	31	41	194	251	474	599
sub09	41	NaN*	275	-	509	-
sub10	17	6	126	36	299	143

* NaN means no pain is detected during the stimulation.

D. Leave-One-Subject-Out Cross-Validation (LOSOCV)

In order to study the performance of the proposed approach, especially the stability of the algorithm across different subjects, a leave-one-subject-out cross-validation (LOSOCV) [30] was adopted. Each time, only one patient's dataset D^i was used as the test set while all others' data D^{i^*} as the training set, where $i \cup i^* = \{1, 2, \cdots, N\}$, and N is the number of patients. Mixing one patient's data in both training and test sets would give the algorithm prior knowledge and cause fake high-performance metrics. Hence, LOSOCV is a fair evaluation scheme to truly reveal the robustness of the classifier. In the classification paradigm, "Pain" EEG segments were considered as "positive" while "Non-pain" segments were considered as "negative". Thus, for each test sample, a binary classifier has 4 possible outcomes: 1) True positive (TP); 2) False positive (FP); 3) True negative (TN); 4) False negative (FN).

In practice, for pain detection, due to uncertain factors, e.g., individual difference, recording environment, it is challenging to keep the sample balance for different subjects. In order to avoid the fake high accuracy which might be produced by sample unbalance, the receiver operating characteristic (ROC) curve was employed to evaluate the algorithm performance in this study. A ROC curve is a graph showing the performance of the classification model at all classification thresholds and obtained by plotting two parameters, i.e., True Positive Rate (TPR), False Positive Rate (FPR). True Positive Rate (TPR) and False Positive Rate (FPR) are defined as: $TPR = \frac{TP}{TP+FN}$, and $FPR = \frac{FP}{FP+TN}$.

A ROC curve plots TPR versus FPR at different classification thresholds. Lowering the classification threshold classifies more items as positive, thus increasing both FPs and TPs. With ROC, we can use the Area under the ROC Curve (AUC) as the performance metric. AUC measures the entire two-dimensional area underneath the entire ROC curve from $(0, 0)$ to $(1, 1)$. In general, the higher the AUC, the better the

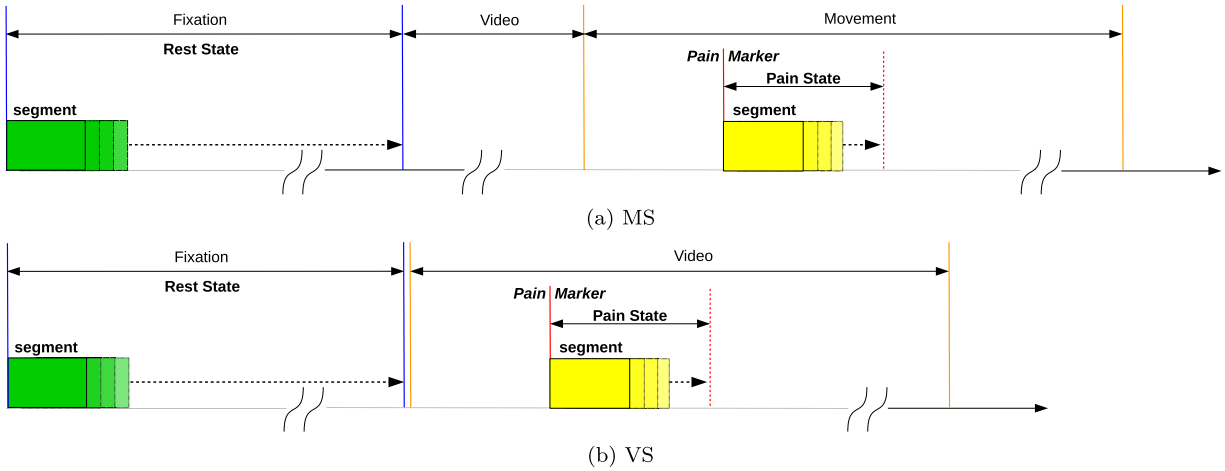

Fig. 5. **EEG segmentation in MS and VS.** In MS and VS, the two blue lines range the fixation stage, while the two orange lines range the pain stimulation stage. In each stimulation, when a pain is marked (red line), the 10s after the "Pain Marker" is extracted as a pain state segment (yellow block). In the fixation stage, a 5s sliding window is used to extract the rest state segment (green block). In MS, pain occurs during the movement. In VS, pain occurs during the video play.

classification model. In this study, AUC was employed as the performance metric to evaluate the algorithm's ability to distinguish "Non-pain" and "Pain" EEGs.

In general, an AUC of 0.5 suggests no discrimination (i.e., ability to distinguish positive and negative samples), 0.7 to 0.8 is considered acceptable, 0.8 to 0.9 is considered excellent, and more than 0.9 is considered outstanding [31].

E. Convolutional Neural Network

In this study, the proposed pain detector was made of CNN. The multi-layers CNN model structure is illustrated in Fig. 6. The network is in reference to previous researches to use CNN in EEG decoding, including, DeepConvNet, ShallowConvNet [26], and EEGNet [25].

The input to the CNN structure is the bandpass filtered 32-channel scalp EEG. A CNN predictor was trained to assign the input segment X^j a class label, i.e., $f(X^j;\theta) \in \mathbb{R}^{C.T} \rightarrow \mathbb{R}^P$, where θ is the parameter set of CNN, $C = 32$ is the number of channels, $T = 250 \times 5 = 1250$ is the time points, and $P \in \{0, 1\}$ is the possible output label. The model contains 5 convolutional layers, a batch normalization layer, and a 2D max-pooling layer. The first two convolutional layers correspond to the temporal filtering and spatial filtering of the EEG segment. In the first layer, each filter performs a convolution over time, while in the second layer, each filter performs spatial filtering with weights for all possible pairs of electrodes with filters of the preceding temporal convolution. After each max-pooling layer, a 30% dropout is used to avoid over-fitting. As the model is designed for a binary classification problem, the last dense layer is set with sigmoid activation function $S(z) = 1/(1 + e^{-z})$, where z is the dense output of the last dropout layer (L17). Then the entire CNN classifier is trained to assign high probabilities to the correct labels by minimizing the sum of the per-example losses: $\theta^* = \underset{\theta}{argmin} \Sigma_{j=1}^{L} loss(y^j, f(X^j;\theta))$, where L is the number of segments in the training set, and $loss$ is the loss function which is binary cross-entropy in this work. The binary cross-entropy (BCE) is for input X^j is defined as:

$$BCE(X^j) = \frac{\sum_{i=1}^{2}(y_i log(f(X^j;\theta)) + (1-y_i) log(1-f(X^j;\theta)))}{2}$$

where y_i is the true label.

A grid search of optimizers and activation functions is employed in this work to create the CNN model which implies that selection of hyper-parameters selection is done exhaustively. Considered options of optimizers include, "SGD", "RMSprop", and "Adam" whereas options of activations include, "elu", "relu", and "tanh". Only the optimal parameter set is retained to build up the pain detector. The details of optimizer and activation functions can be found at work [23], https://keras.io/api/optimizers/ and https://keras.io/api/layers/activations/. To construct the model, Python3.7 and Keras2.2.4 (https://keras.io/) are employed in this work.

IV. Results and Discussion

Our motivation is to investigate the performance of CNN for the benefit of EEG-based pain detection, which has high potential in clinical research and solutions. As indicated in the previous sections, the scalp EEG was employed as the input of a multi-layer CNN pain detector. The following subsections will demonstrate the classification results of pain detection based on CNN and compare our approach with respect to the state-of-the-art, in both MS and VS phases. In addition, the 32 channels will also be divided into several scalp areas to explore the significance of brain areas while detecting pain.

A. Pain Detection in MS

While classifying the "Pain" and "Non-pain" segments in the MS phase of all 10 patients, a consistent AUC over 0.70 was obtained across all patients. The average AUC is

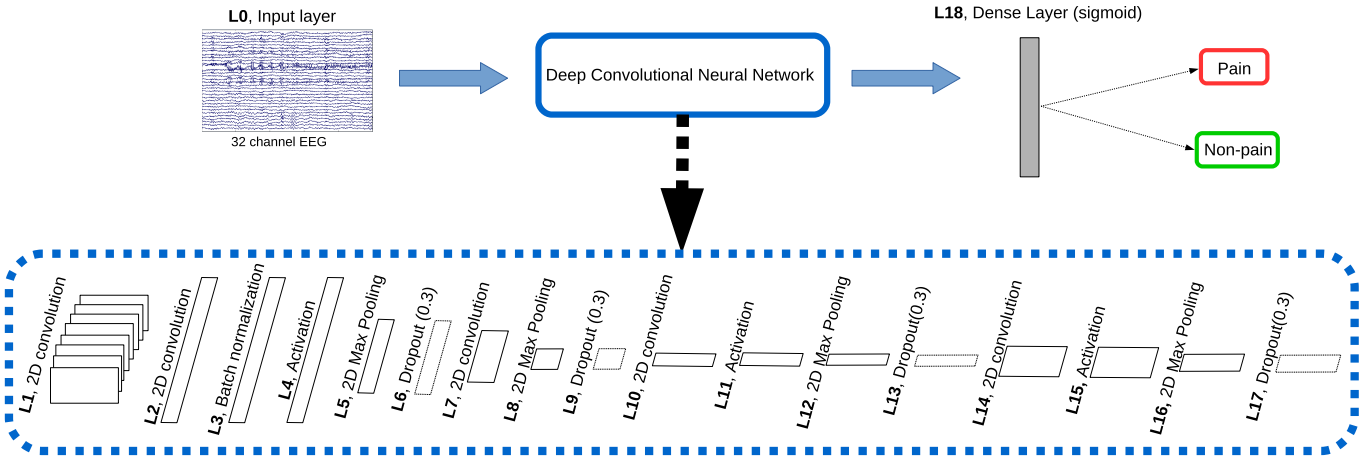

Fig. 6. **Network structure.** The input is multi-channel EEG segment with a dimension 32(*channel*) × 1250(*sampling point*, 5 × 250). L1 is a temporal filter that contains 25 filters with a 1 × 10 kernel. L2 is a spatial filter that contains 25 filters with a 32 × 1 kernel. In L5, L8, L12, and L16, the pool size is (1, 3) and the stride is (1, 3). L7 contains 50 filters with 1 × 10 kernels. L10 contains 100 filters with a 1 × 10 kernel. L14 contains 200 filters with a 1 × 10 kernel. L18 is a dense layer with sigmoid activation whose output is the predicted class, i.e., "Pain" or "Non-pain". A grid search of optimizer and activation function (L4, L11, L15) is utilized to investigate the optimal hyper-parameter settings.

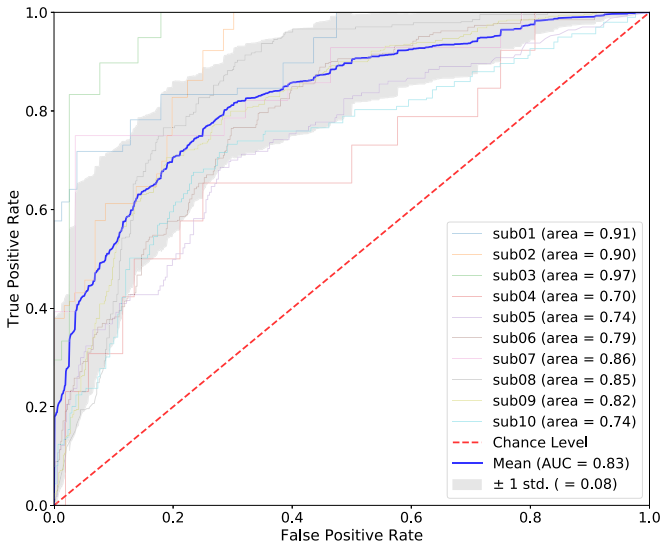

Fig. 7. **ROC of LOSOCV (MS).**

0.83 which is very promising. Because we use leave-one-subject-out cross-validation, the robustness of our approach to overcoming individual differences is proven. To specifically illustrate the performance metric, we visualize the individual and averaged ROC curves together in Fig. 7. The transparent lines represent the ROC curve of each patient. The bold blue line is the average ROC curve across the ten subject-specific ROC curves. The confidence intervals with ±1 std are represented by the grey area. The model providing the highest AUC for each patient in a grid search of optimizer and activation function is illustrated here and later in VS. "SGD" is the employed optimizer and "elu" is the activation function, after grid search in MS.

As seen in Fig. 7, ROC curves of all patients show a consistent pattern that the AUC of each patient (transparent lines) is much higher than the chance level (red dashed line). The highest AUC is 0.97 for sub03. The lowest AUC is 0.70 for sub04 which is still much higher than the chance level (red dashed line). Also, it can be seen that six in ten patients achieve AUCs above 0.80.

It is worth mentioning that there are two options of AUC averaging in cross-validation, one is to calculate one ROC and one AUC per fold, then generate a numerical average AUC, the other is to integrate the probabilities of all folders to make one ROC and one merged AUC. In this work, we recommend the first way and make the analysis accordingly for two reasons. First, option 1 provides the AUC variance, which is very significant in cross-validation, with a visual impression of the uncertainty of the test result on each subject. Second, a well-calibrated probability estimation across subjects is hard to guarantee, may lead to an unintended problem by sorting probabilities of different subjects together. However, considering the analyzing preference, we still report the merged AUC here for reference. In MV, the merged AUC is 0.70.

B. Pain Detection in VS

In VS phase, individual and averaged ROC curves are illustrated in Fig. 8. The transparent lines represent the ROC curve of each patient and the bold blue line is the average ROC curve across 10 patients. The confidence intervals with ±1 std indicate the grey area. The average AUC of our approach achieved on VS was very close to that on MS. However, the individual AUC on VS differed from that on MS. The highest AUC is at 1.00 for sub03. The lowest AUC is 0.59 for sub06, slightly higher than the chance level. The difference can be seen by comparing the patterns in Figs. 7 and 8. In VS, the algorithm produced low AUC on two patients (sub06: 0.59, sub07: 0.66), while in MS, the AUCs of sub06 and sub07 are both above 0.80. In contrast, the AUCs of sub03, sub04, sub05, and sub10 on VS are higher than that on MS, especially for sub04 and sub10 (15% higher). However, the average AUC (0.81) in VS was very close to that on MS,

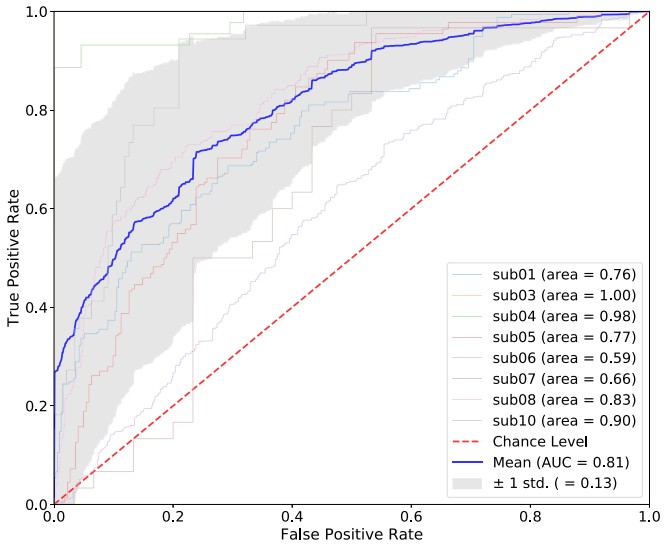

Fig. 8. **ROC of LOSOCV (VS)**.

proving the stability of the proposed method in pain detection under VS. It is worth noting that there might be two reasons for the subject-specific AUCs under both stimulations. First, the individual difference can create significant classification bias across patients, either in MS or VS. Secondly, the pain EEG pattern may switch under different stimulations. Such a difference can be explained more in a further discussion in Section IV-D, which focuses on distinct brain areas affecting pain detection. Similar to MV, we also give the merged AUC in VS here, which was 0.63.

C. Comparison With State-of-the-Art

Although the proposed method achieved good pain detection results, it is worth investigating whether it is significantly better than existing methods. Since there is very limited work available in the literature for machine-learning-based chronic pain detection based on EEG, the proposed method was compared with three recently published machine-learning-based approaches inducing thermal pain [6], [20], and cold presser pain [32]. In Misra *et al.* [6], SVM was used to automatically classify EEG data into low- and high-pain classes. Theta and gamma power in the medial prefrontal area and lower beta power in the contralateral sensorimotor area served as features for classification. In Vijayakumar *et al.* [20], a random forest model was trained to predict pain scores using time-frequency wavelet representations of independent components obtained from electroencephalography (EEG) data, and the relative importance of each frequency band to pain quantification is assessed. In Nezam *et al.* [32], SVM was used for pain EEG classification under the feature space which contains band power, fractal dimension, Shannon entropy, approximate entropy, and spectral entropy. In addition, the proposed method is compared with the latest deep-learning-based EEG analysis tools, including, DeepConvNet, ShallowConvNet [26], and EEGNet [25]. For random forest in Vijayakumar *et al.* [20], "gini" was selected as the criterion, while grid search was used for the optimization of the number of trees, maximum depth, and minimum samples split, in set, [50, 100, 150, 200], [1, 3, 5, 7, 9, 11], and [20, 40, 60, 80]. For SVM in Misra *et al.* [6] and Nezam *et al.* [32], the best settings were obtained from grid search of gamma and c, in set $[10^{-2}, 10^{-1}, 10^{0}, 10^{1}, 10^{2}]$. For DeepConvNet, ShallowConvNet, and EEGNet, the same grid search of optimizers and activation functions as in Section III-E employed.

The comparison of AUC values for different methods on MS and VS are listed in Tables II and III, respectively.

Our approach outperformed the other methods by delivering significantly higher average AUCs than the existing methods, in both stimulations. In MS phase EEG classification, compared with our approach, AUC offered by Misra *et al.* [6] was slightly better for sub10, while Vijayakumar *et al.* [20] achieved higher AUC for sub02, sub03, sub04, and sub07. However, the proposed CNN model achieved much better overall performance on average. For Misra *et al.* [6], the AUCs of 6 (sub01, sub04, sub05, sub06, sub07, and sub09) in 10 patients were lower than 0.70, indicating very limited discrimination ability for pain detection. The model of Vijayakumar *et al.* [20] was slightly better than that of Misra *et al.* [6] on average AUC, but still generated AUCs lower than 0.70 in 4 subjects, namely sub01, sub05, sub06, and sub10. An interesting finding is, it is much more difficult to detect the pain EEG for some subjects than the others, especially on sub01, sub05, and sub06 by the existing approaches. Though Misra *et al.* [6] and Vijayakumar *et al.* [20] have their pros and cons across subjects, they showed very limited classification capabilities in dealing with sub01, sub05, and sub06. In comparison, our approach obtained much higher AUCs on these three and gained at least 0.14 improvement on average. In addition, our approach did not create significant bias among subjects. In other words, the AUCs of the patients were all higher than 0.70. Six out of ten patients were even higher than 0.80, considering the promising discrimination capability of the proposed method. Furthermore, our approach achieved a much higher average AUC and a much lower standard deviation than the other two methods, proving better algorithm robustness across subjects in MS. When compared with the three state-of-the-art deep-learning-based methods, our approach still achieved much better performance. Among the three methods, DeepConvNet obtained the best classification result, which was also the closest to this work but is still two percentage points lower. At the same time, its std is 5 percentage points higher than that of the proposed method.

In VS, compared with the proposed approach, the methodology reported in Misra *et al.* [6] achieved higher AUC in sub05 whereas Vijayakumar *et al.* [20] achieved higher AUC on sub04 and sub05. However, across 10 subjects, the average AUC was less than that in the proposed method. For Misra *et al.* [6], the AUCs of 6 (sub01, sub03, sub06, sub07, sub08, and sub09) out of 8 patients were lower than 0.70, indicating unacceptable accuracy in pain detection. Besides, for sub03, sub06, and sub08, the AUCs were even lower than the chance level. AUC offered by Vijayakumar *et al.* [20] was slightly better than Misra *et al.* [6] for sub01, sub06, sub08, and sub10, but offered lower AUCs than 0.70 for 3 subjects: sub03, sub06, and sub07. The AUCs offered by

TABLE II
METHOD COMPARISON (MS)

MS	**This Work**	Gaurav et al. [6]	Vishal et al. [20]	Tahereh et al. [32]	EEGNet [25]	DeepConvNet [26]	ShallowConvNet [26]
sub01	0.91	0.07	0.64	0.96	0.93	0.94	0.94
sub02	0.90	0.86	0.92	0.50	0.91	0.91	0.85
sub03	0.97	0.71	1.00	0.81	0.89	1.00	0.93
sub04	0.70	0.51	0.74	0.53	0.90	0.70	0.70
sub05	0.74	0.54	0.52	0.72	0.54	0.56	0.68
sub06	0.79	0.65	0.46	0.72	0.55	0.70	0.71
sub07	0.86	0.51	1.00	0.88	0.88	0.98	0.79
sub08	0.85	0.79	0.77	0.81	0.53	0.82	0.66
sub09	0.82	0.60	0.76	0.80	0.76	0.78	0.69
sub10	0.74	0.77	0.51	0.88	0.76	0.75	0.71
Average	$\mathbf{0.83 \pm 0.09}$	$\mathbf{0.60 \pm 0.22}$	$\mathbf{0.73 \pm 0.20}$	$\mathbf{0.76 \pm 0.15}$	$\mathbf{0.76 \pm 0.16}$	$\mathbf{0.81 \pm 0.14}$	$\mathbf{0.76 \pm 0.10}$

TABLE III
METHOD COMPARISON (VS)

VS	**This Work**	Gaurav et al. [6]	Vishal et al. [20]	Tahereh et al. [32]	EEGNet [25]	DeepConvNet [26]	ShallowConvNet [26]
sub01	0.76	0.67	0.73	0.74	0.56	0.68	0.74
sub03	1.00	0.49	0.22	0.96	0.77	0.63	0.92
sub04	0.98	0.97	1.00	0.98	0.93	0.94	0.99
sub05	0.77	0.81	0.92	0.80	0.56	0.60	0.76
sub06	0.59	0.47	0.52	0.50	0.51	0.56	0.59
sub07	0.66	0.51	0.47	0.50	0.58	0.57	0.55
sub08	0.83	0.44	0.73	0.50	0.64	0.67	0.62
sub10	0.90	0.55	0.72	0.85	0.85	0.75	0.76
Average	$\mathbf{0.81 \pm 0.15}$	$\mathbf{0.62 \pm 0.19}$	$\mathbf{0.66 \pm 0.25}$	$\mathbf{0.73 \pm 0.21}$	$\mathbf{0.67 \pm 0.12}$	$\mathbf{0.76 \pm 0.10}$	$\mathbf{0.74 \pm 0.15}$

TABLE IV
TRAINING TIMES

	This Work	Gaurav et al. [6]	Vishal et al. [20]	Tahereh et al. [32]	EEGNet [25]	DeepConvNet [26]	ShallowConvNet [26]
MS	138,288	81,565	49,834	10,373	148,255	122,684	80,647
VS	93,259	69,796	39,166	7,060	100,522	82,906	71,923

* Training times are given in seconds.

Vijayakumar *et al.* [20] for sub03 and sub07 were even lower than the chance level. Like in MS, it is much more challenging to detect the pain EEG accurately for some subjects than the others, especially on sub03, sub06, and sub07. Existing methods did not perform well in the classification of pain states in sub03, sub06, and sub07. In comparison, our approach obtained much higher AUCs on sub03, sub06, and sub07. On sub06 and sub07, the AUCs were at least 0.07 higher. On sub03, either Misra *et al.* [6] or Vijayakumar *et al.* [20] gave AUCs lower than the chance level, while the proposed algorithm offered 100% classification accuracy. Though AUCs of sub06 and sub07 by the proposed method were still lower than 0.70, the average AUC was relatively much higher than the other two methods. Moreover, our approach achieved a much lower standard deviation than the other two methods, proving better algorithm robustness across subjects in VS. It is worth noting that the pain EEG detection in VS is more difficult than that in MS, which can be peered from several aspects. First, for our approach and Misra *et al.* [6], the ratio of subjects that achieve AUCs lower than 0.70 in VS is significantly higher than that in MS. The AUCs of all the patients were higher than 0.70 in MS, while 2 in 8 subjects were lower than 0.70 in VS when using our approach. This ratio increased to $6/10$ in MS and $6/8$ in VS when using Misra *et al.* [6]. Second, using either our approach or Vijayakumar *et al.* [20], the average AUC decreased, especially for Vijayakumar *et al.* [20], which drops to 0.66, worse than the lower boundary of acceptable AUC, 0.70. When compared with the three state-of-the-art deep-learning-based methods, our approach achieved at least 5 percentage points higher at AUC. In the state-of-the-art methods based on CNN, DeepConvNet obtained the best classification result. However, in all the 8 subjects, the prediction results of DeepConvNet were lower than that of our method. Similar comparison results also exist for EEGNet and ShallowConvNet.

Although the proposed method obtains the highest AUC among all methods, the computational cost is another important indicator that needs to be considered. Table IV lists the computational time of all the methods. For the fairness of comparison, training times are end-to-end, that is, including the loading and preprocessing of the data. The methods based on SVM and random forest were substantially faster to train than the CNN-based methods. It is worth mentioning that these times are only meant to give a rough estimate of the training times as there were differences in the computing environment, especially between CNN-based classifiers and traditional machine-learning classifiers. Most importantly, Misra *et al.* [6], Vijayakumar *et al.* [20], and Nezam *et al.* [32] were trained on CPU, while our method, EEGNet [25], DeepConvNet [26], and ShallowConvNet [26] were trained on GPUs.

In general, the proposed method produced much better pain detection performance than the other methods, obtaining the highest value of AUCs in both MS and VS, proving its good stability to handle pain detection under different stimulations. Compared with the methods based on traditional classifiers,

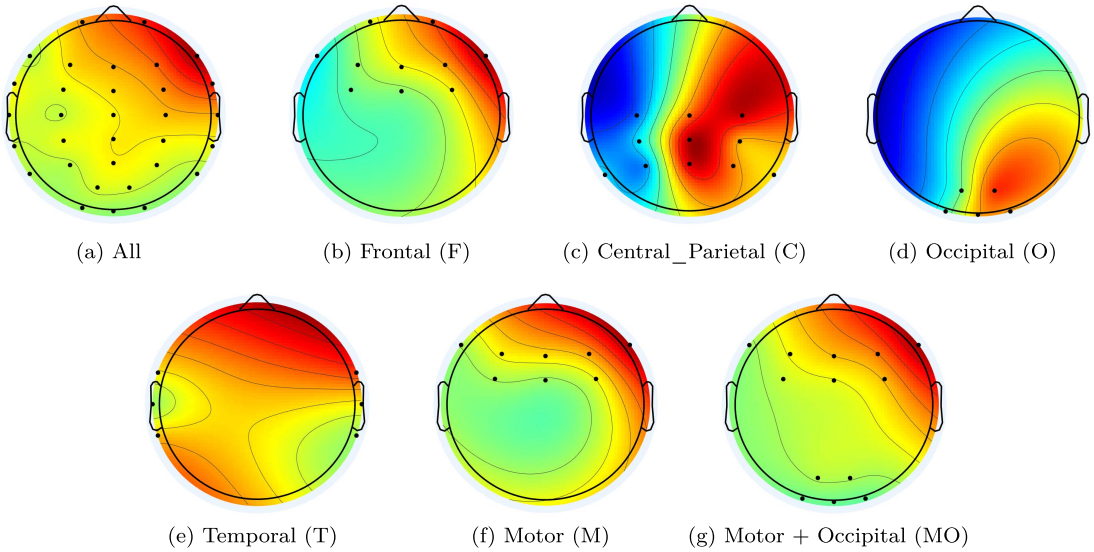

Fig. 9. **EEG electrodes of brain areas**.

e.g., SVM, random forest, the CNN-based approach can reduce the manual intervention, making the classification model relatively easier to be implemented. Besides, the proposed method can extract the temporal (L1) and spatial (L2) information from the raw signal much more efficiently.

D. Significance of Brain Areas

Unlike other sensations associated with specific areas in the brain, such as vision, touch, and hearing, it is hard to find studies reporting specific cortical area activations dedicated to pain with different kinds of stimulations. Hence, it will be beneficial for pain research to explore brain areas significantly involved in pain generation in both types of stimulation. Here, a brief discussion on the detection in different brain areas under MS and VS is presented. The 32 channels are divided into 6 areas as follows:

- Frontal (F): Fp1, Fp2, F3,Fz,F4, F7, F8, FC3, FCz, FC4
- Central_Parietal (C): C3, Cz, C4, CP3, CPz, CP4, P3, PZ, P4, P7,P8
- Occipital (O): PO1, PO2, O2, Oz, O2
- Temporal (T): FT7, FT8, T7, T8, TP7, TP8
- Motor (M): F3,Fz,F4, F7, F8, FC3, FCz, FC4
- Motor_Occipital (MO): F3,Fz,F4, F7, F8, FC3, FCz, FC4, PO1, PO2, O2, Oz, O2

The 6 areas are named as Frontal (F), Central-Parietal (C), Occipital (O), Temporal (T), Motor (M), and Motor-Occipital (MO), including the channels. Fig. 9 shows the locations of electrodes in each area. The CNN model providing the highest AUC in a grid search of optimizers and activation functions (as in Section IV-A and Section IV-B) is used here to investigate brain areas for both MS and VS phases. The sequel explains the significance of different brain areas in EEG-based pain detection under MS and VS separately in line with the previous subsections.

Table V provides the AUC values in pain detection for each brain area for the MS phase. Comparing different areas, the main finding in MS is that the average AUCs obtained in different areas are very close. The highest AUC, 0.84, was in the motor + occipital (MO), while the lowest AUC, 0.80, was in the temporal (T). This indicated that all the brain areas are evoked when pain occurs in actual movement. Under the MS, any independent brain area is sufficient to guarantee a reliable detection AUC using the proposed approach. Besides, area "MO" outperformed "All" in 6 of the 10 patients. The average AUC of "MO" was the highest among the brain areas. The motor cortex is the control and execution center of voluntary movements. While the occipital lobe is the visual processing center of the brain containing most of the anatomical area of the visual cortex. So, it makes sense that using the MO area can achieve even better pain detection results than involving all the channels. Nevertheless, the selection of a sub-brain area can efficiently reduce the computational cost, especially in the CNN model.

Though the average AUCs of different brain areas were very close in a single subject, the AUCs vary among different subjects. When the detection was based on the whole brain, the AUCs of all the subjects were higher than 0.70. In comparison, the AUCs of certain subjects were lower than the lower

TABLE V
BRAIN AREAS SIGNIFICANCE (MS)

	All	F	C	O	T	M	MO
sub01	0.91	0.94	0.81	0.98	0.85	0.94	0.99
sub02	0.90	0.97	0.98	0.91	0.89	0.94	0.94
sub03	0.97	0.97	0.92	0.85	0.98	0.88	0.94
sub04	0.70	0.82	0.90	0.73	0.83	0.73	0.71
sub05	0.74	0.70	0.67	0.77	0.65	0.72	0.77
sub06	0.79	0.63	0.67	0.72	0.65	0.65	0.75
sub07	0.86	0.98	0.83	0.88	0.91	0.99	0.99
sub08	0.85	0.84	0.87	0.74	0.83	0.79	0.75
sub09	0.82	0.75	0.70	0.85	0.70	0.69	0.82
sub10	0.74	0.73	0.73	0.87	0.69	0.74	0.75
Average	**0.83**	**0.83**	**0.81**	**0.83**	**0.80**	**0.81**	**0.84**

* All: 32 channels; F: frontal; C: central; O: occipital; T: temporal; M: motor; MO: motor + occipital

TABLE VI
BRAIN AREAS SIGNIFICANCE (VS)

	All	F	C	O	T	M	MO
sub01	0.76	0.63	0.62	0.88	0.75	0.71	0.79
sub03	1.00	0.84	0.96	0.96	0.86	0.81	1.00
sub04	0.98	0.98	1.00	0.97	0.98	1.00	0.99
sub05	0.77	0.77	0.71	0.76	0.66	0.74	0.79
sub06	0.59	0.55	0.60	0.55	0.58	0.57	0.56
sub07	0.66	0.62	0.66	0.79	0.49	0.58	0.64
sub08	0.83	0.71	0.73	0.77	0.77	0.76	0.81
sub10	0.90	0.68	0.83	0.87	0.57	0.74	0.80
Average	**0.81**	**0.72**	**0.76**	**0.82**	**0.71**	**0.74**	**0.80**

* All: 32 channels; F: frontal; C: central; O: occipital; T: temporal; M: motor; MO: motor + occipital

boundary of acceptable AUC (0.70) in several brain areas, such as frontal of sub06, central of sub05 and sub06, etc. This phenomenon proves that the algorithm robustness varies in different brain areas across subjects. In addition, while comparing areas O and M, it is found that O performed well on all subjects, but sub06 and sub09 generate AUCs lower than 0.70 in M. This indicates that a relatively stronger activation is evoked in area O than that in area M. The algorithm can capture enhanced EEG pattern for pain detection by combining areas O and M.

The results of pain detection under different brain areas in VS are listed in Table VI. It is observed that AUCs obtained across 10 subjects over the different scalp areas are much more scattered than that in MS. On average, the highest AUC was 0.82 in occipital (O), whereas the lowest AUC was only 0.71 in temporal (T). This indicates that, compared with MS, VS activates a partial activation for pain EEG in a relatively smaller area than MS. It may be because of the fact that MS evokes pain EEG over relatively larger brain areas than that in VS. MS assigns multiple lobes for task execution, such as the occipital lobe for visual processing and motor cortex for the control and execution of voluntary movements. In contrast, VS is most likely to directly stimulate the occipital area when the patient concentrates on the video played in the front. Besides, the average AUC of "O" is slightly better than "All", which is also the highest among all the areas in VS. As we explained previously, the occipital lobe is the visual processing center of the brain, so it is not surprising that area "O" achieves even higher AUC than that obtained using all the channels. Meanwhile, the area "O" only occupied 5 EEG channels, significantly reducing the computational cost.

The advantage of area "O" was reflected in its highest average AUC and in the better performance on each subject. While using all the 32 channels, the AUCs of 2 (sub06 and sub07) out of 8 subjects were lower than 0.70. This number was dropped to 1 (only sub06) in area O. Furthermore, compared with "O" and "All", area "O" had a significant AUC improvement at 0.12 and 0.13, on sub01 and sub07, respectively.

If the conditions are insufficient for brain area selection in pain detection, e.g., limited channels, unknown evoking areas, the safest way for EEG-based pain detection is to employ all EEG channels. However, if the stimulation and the activation area(s) are evident, a subset of channels covering specific brain areas should be considered for achieving better detection accuracy at a lower computational cost. Results in this work may provide a new solution and insights for researchers and clinical practitioners for pain detection.

V. CONCLUSION

Identifying neurological markers that predict individual predisposition to pain is critical in developing chronic pain treatments and resolving the knowledge of how pain signals are analyzed in the brain. Recent advances in neuroimaging techniques and machine learning algorithms have significantly enhanced ongoing research on pain detection. Our study investigated the detection of pain using EEG in chronic back pain patients employing deep CNN architecture. The pain was induced among patients under two distinct modes, namely, movement stimulation (MS) and video stimulation (VS). Meanwhile, the associated EEG oscillations were continuously recorded. Using the proposed multi-layer network model, robust performance for classifying EEG "Pain" and "Non-pain" EEG segments was achieved, with AUCs higher than 0.80. In addition, the brain areas evoked under MS and VS were analyzed. In MS, motor and occipital lobes contributed to the highest AUC values in detection. In contrast, the occipital lobe contributed to the highest AUC in VS. Further research will be needed to validate further the current results with data obtained from a bigger and wider sample of patients with chronic pain. Applying novel EEG paradigms and methodologies will allow us to better understand the mechanisms underlying chronic pain, especially the knowledge of brain activities in this field.

ACKNOWLEDGMENT

The computational work for this project was partially performed on resources of the National Supercomputing Centre, Singapore.

REFERENCES

[1] M. Ploner, C. Sorg, and J. Gross, "Brain rhythms of pain," *Trends Cognit. Sci.*, vol. 21, no. 2, pp. 100–110, Feb. 2017.
[2] M. M. van der Miesen, M. A. Lindquist, and T. D. Wager, "Neuroimaging-based biomarkers for pain: State of the field and current directions," *PAIN Rep.*, vol. 4, no. 4, p. e751, Jul. 2019.
[3] (2020). *Pain Terms: The International Association for the Study of Pain (IASP)*. [Online]. Available: https://www.iasp-pain.org/Education/Content.aspx?ItemNumber=1698#Pain
[4] D. J. Gaskin and P. Richard, "The economic costs of pain in the United States," *J. Pain*, vol. 13, no. 8, pp. 715–724, Aug. 2012.
[5] K. D. Davis *et al.*, "Brain imaging tests for chronic pain: Medical, legal and ethical issues and recommendations," *Nature Rev. Neurol.*, vol. 13, no. 10, pp. 624–638, 2017.
[6] G. Misra, W.-E. Wang, D. B. Archer, A. Roy, and S. A. Coombes, "Automated classification of pain perception using high-density electroencephalography data," *J. Neurophysiol.*, vol. 117, no. 2, pp. 786–795, Feb. 2017.
[7] E. S. D. S. Pinheiro *et al.*, "Electroencephalographic patterns in chronic pain: A systematic review of the literature," *PLoS ONE*, vol. 11, no. Feb, pp. 1–26, Feb. 2016.
[8] S. Ta Dinh *et al.*, "Brain dysfunction in chronic pain patients assessed by resting-state electroencephalography," *Pain*, vol. 160, no. 12, pp. 2751–2765, Dec. 2019.
[9] R. Sitaram *et al.*, "Closed-loop brain training: The science of neurofeedback," *Nature Rev. Neurosci.*, vol. 18, no. 2, pp. 86–100, Dec. 2016.

[10] R. Polanía, M. A. Nitsche, and C. C. Ruff, "Studying and modifying brain function with non-invasive brain stimulation," *Nature Neurosci.*, vol. 21, no. 2, pp. 174–187, Jan. 2018.
[11] M. N. Baliki and A. V. Apkarian, "Nociception, pain, negative moods, and behavior selection," *Neuron*, vol. 87, no. 3, pp. 474–491, Aug. 2015.
[12] J. P. Rauschecker, E. S. May, A. Maudoux, and M. Ploner, "Frontostriatal gating of tinnitus and chronic pain," *Trends Cognit. Sci.*, vol. 19, no. 10, pp. 567–578, Oct. 2015.
[13] D. V. M. *et al.*, "Altered resting state EEG in chronic pancreatitis patients: Toward a marker for chronic pain," *J. Pain Res.*, vol. 2013, no. 6, pp. 815–824, Nov. 2013.
[14] M. P. Jensen *et al.*, "Steps toward developing an EEG biofeedback treatment for chronic pain," *Appl. Psychophysiol. Biofeedback*, vol. 38, no. 2, pp. 101–108, Jun. 2013.
[15] M. P. Jensen *et al.*, "Brain EEG activity correlates of chronic pain in persons with spinal cord injury: Clinical implications," *Spinal Cord*, vol. 51, no. 1, pp. 55–58, Jul. 2012.
[16] S. Vanneste, J.-J. Song, and D. D. Ridder, "Thalamocortical dysrhythmia detected by machine learning," *Nature Commun.*, vol. 9, no. 1, pp. 1–13, Mar. 2018.
[17] A. Mansour *et al.*, "Global disruption of degree rank order: A hallmark of chronic pain," *Sci. Rep.*, vol. 6, no. 1, Oct. 2016, Art. no. 34854.
[18] A. Mouraux and G. D. Iannetti, "The search for pain biomarkers in the human brain," *Brain*, vol. 141, no. 12, pp. 3290–3307, Dec. 2018.
[19] E. Schulz, A. Zherdin, L. Tiemann, C. Plant, and M. Ploner, "Decoding an individual's sensitivity to pain from the multivariate analysis of EEG data," *Cerebral Cortex*, vol. 22, no. 5, pp. 1118–1123, May 2011.
[20] V. Vijayakumar, M. Case, S. Shirinpour, and B. He, "Quantifying and characterizing tonic thermal pain across subjects from EEG data using random forest models," *IEEE Trans. Biomed. Eng.*, vol. 64, no. 12, pp. 2988–2996, Dec. 2017.
[21] D. Borsook, S. Sava, and L. Becerra, "The pain imaging revolution: Advancing pain into the 21st century," *Neuroscientist*, vol. 16, no. 2, pp. 171–185, Apr. 2010.
[22] I. Tracey, "Can neuroimaging studies identify pain endophenotypes in humans?" *Nature Rev. Neurol.*, vol. 7, no. 3, pp. 173–181, Mar. 2011.
[23] Y. LeCun, Y. Bengio, and G. Hinton, "Deep learning," *Nature*, vol. 521, pp. 436–444, May 2015.
[24] W.-Y. Hsu, "Fuzzy Hopfield neural network clustering for single-trial motor imagery EEG classification," *Expert Syst. Appl.*, vol. 39, no. 1, pp. 1055–1061, Jan. 2012.
[25] V. J. Lawhern, A. J. Solon, N. R. Waytowich, S. M. Gordon, C. P. Hung, and B. J. Lance, "EEGNet: A compact convolutional neural network for EEG-based brain–computer interfaces," *J. Neural Eng.*, vol. 15, no. 5, Jul. 2018, Art. no. 056013.
[26] R. T. Schirrmeister *et al.*, "Deep learning with convolutional neural networks for EEG decoding and visualization," *Hum. Brain Mapping*, vol. 38, pp. 5391–5420, Nov. 2017.
[27] D. Sussillo, S. D. Stavisky, J. C. Kao, S. I. Ryu, and K. V. Shenoy, "Making brain–machine interfaces robust to future neural variability," *Nature Commun.*, vol. 7, no. 1, Dec. 2016, Art. no. 13749.
[28] M. Leeuw, M. E. J. B. Goossens, G. J. P. van Breukelen, K. Boersma, and J. W. S. Vlaeyen, "Measuring perceived harmfulness of physical activities in patients with chronic low back pain: The photograph series of daily activities—Short electronic version," *J. Pain*, vol. 8, no. 11, pp. 840–849, Nov. 2007.
[29] H. Dong, A. Supratak, W. Pan, C. Wu, P. M. Matthews, and Y. Guo, "Mixed neural network approach for temporal sleep stage classification," *IEEE Trans. Neural Syst. Rehabil. Eng.*, vol. 26, no. 2, pp. 324–333, Feb. 2018.
[30] C. Jiang, Y. Li, Y. Tang, and C. Guan, "Enhancing EEG-based classification of depression patients using spatial information," *IEEE Trans. Neural Syst. Rehabil. Eng.*, vol. 29, pp. 566–575, 2021.
[31] J. N. Mandrekar, "Receiver operating characteristic curve in diagnostic test assessment," *J. Thoracic Oncol.*, vol. 5, no. 9, pp. 1315–1316, Sep. 2010.
[32] T. Nezam, R. Boostani, V. Abootalebi, and K. Rastegar, "A novel classification strategy to distinguish five levels of pain using the EEG signal features," *IEEE Trans. Affect. Comput.*, vol. 12, no. 1, pp. 131–140, Jan. 2021.